

## ON-OFF BOILER, THERMAL STORAGE AND SOLAR COLLECTOR: ENERGY BALANCE BASED MODEL AND ITS OPTIMIZATION

Milica Grahovac<sup>1</sup>, Petra Liedl<sup>2</sup>, Jérôme Frisch<sup>3</sup>, Peter Tzscheuschler<sup>1</sup>

<sup>1</sup> Lehrstuhl für Energiewirtschaft und Anwendungstechnik, [mgrahovac@tum.de](mailto:mgrahovac@tum.de)

<sup>2</sup> Lehrstuhl für Bauklimatik und Haustechnik

<sup>3</sup> Lehrstuhl für Computation in Engineering

International Graduate School of Science and Engineering (IGSSE)

Technische Universität München

### ABSTRACT

A simplified model of a primary HVAC system comprising an on-off boiler, thermal storage and solar thermal collectors is simulated in hourly resolution. The simulation passes the results to an optimization algorithm that sizes the system. The objective is to minimize total costs and reach a desired solar ratio. Results show good model performance and short simulation run time. A global bounded Nelder-Mead method is implemented to calculate optimal system configurations in two case studies.

The amount of user input data is minimised to enable optimal plant configuration selection during early building design, but also to avoid the system oversize.

### INTRODUCTION

One of the most promising measures in energy saving and lowering a carbon footprint of a building is the reduction of HVAC energy consumption. The measures to reduce the consumption should be introduced at the beginning of the building design, parallel to other planning processes. Numerous measures of improvement of the building envelope will decrease the demand but only occasionally completely remove it. The next step towards lower primary energy consumption is to increase the efficiency of the distribution and emission system – the secondary HVAC. Finally, the efficiency of the primary HVAC system, the energy generation plant, needs to be improved. With this work we address the primary HVAC design.

We develop a series of preconfigured simplified primary HVAC models with the main purpose to compare the costs for the alternative designs. Using weather data and an ideal heating or cooling load provided by numerous simulation tools, the model simulates the plant performance and sizes the components utilizing an optimization procedure. The optimization objectives are annual costs during the calculation period, emissions, fuel consumption and utilization of renewables, as well as their combinations. The simulation is quasi-stationary and yearly, with the hourly resolution, which enables thermal storage consideration. The plant models are energy balance based and deal only with loads, but

the inertia of thermal systems has been taken into account by allowing limited short term load shifting. Due to these simplifications, various boundary conditions have been applied in order to comply with the physical laws and thermodynamics of the system. Similar approach is seen in Fabrizio et al. (2009), which does not utilise thermal storage. Sakurai et al. (2007) have developed a tool to assist the early choice of a heating system which doesn't perform component size optimization. Optimization and price comparison of hybrid power systems using time series data is possible with the energy modelling software HOMER (Lambert et al., 2005).

Available tools for primary HVAC design range from those based on procedures prescribed by national standards, to detailed simulation tools, such as e.g. TRNSYS and EnergyPlus, which demand too much input for early design phases. Several tools providing help during conceptual design have been developed, ranging from quantitative, such as CIBSE RESET tool (CIBSE TM38, 2006), which provides evaluation of renewable energy potential depending on the location, to more sophisticated design aid tools, such as eQuest (Hirsch, 2006), the DOE-2 based software.

A simulation model and optimization of a primary heating system comprising an on-off boiler, thermal storage and solar thermal collectors is presented in this paper. The model performance and control strategy is explained and illustrated. The system is sized with regard to total costs and/or utilisation of solar energy, the so-called solar ratio. Optimization is performed using globalised bounded Nelder-Mead method and exhaustive search method. Results are investigated using parameter sensitivity analyses. Optimal system configurations have been calculated using ideal heating loads for two building sizes in Moscow and Shanghai climate. For all the results shown, the supply task has been satisfied. The only case that penalized the solar constraint is the B building in Moscow with the objective to reach the solar ratio of 30%. Utilizing the maximal available roof area, the solar ratio of only 16.5% is achieved, and the penalty has forced the increase in storage volume, which prolonged the boiler operation hours causing the emissions to rise. For Shanghai climate, where the solar gains are higher, the boiler design power and emissions decrease with the increase in

solar ratio is as expected. Since the model demands a minimal amount of input data, its utilisation during early design could be beneficial in terms of choosing the appropriate plant configuration, but also avoiding the oversizing of the system. This is gaining importance with the increased utilization of complex hybrid systems, due to the difficulty in experience-based initial dimensioning.

## MODEL AND SIMULATION

Optimal system component sizes are the result of the optimization algorithm application to the objective function, which is defined by the system performance simulation, see Fig 1.

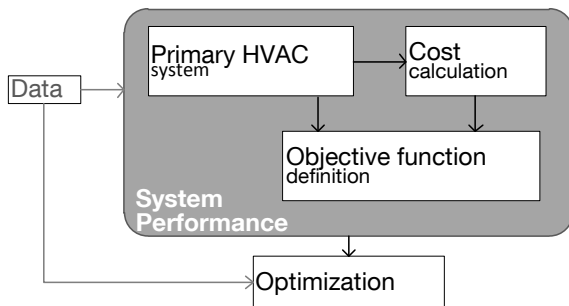


Figure 1 Basic data flow of the simulation and optimization process

System performance model comprises the model of the primary HVAC system we wish to optimize, the calculation of the costs and the definition of the objective function. The equipment parameters the optimization of which is presented in this paper are boiler design power, storage volume, storage discharge power, roof area to be covered by solar collectors and the mean solar collector temperature. This chapter describes the performance of the system modelled and assumptions adopted.

### Primary HVAC system model

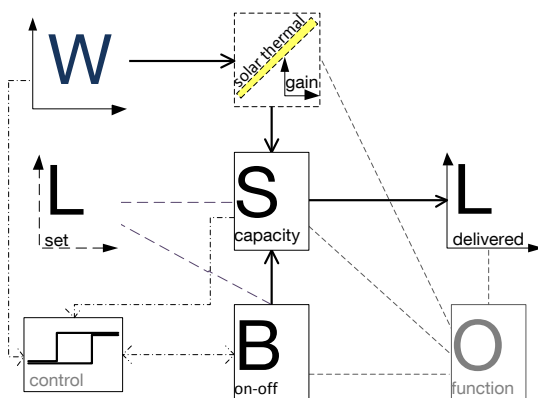


Figure 2 Schematic representation of the modelled system and component interaction. S – storage, B – boiler, L – loads, W – weather data, O – optimization objective

As already stated, the system schematically presented in Figure 2 consists of an on-off boiler, a thermal

storage unit and a solar collector array. Based on the control strategy, the solar collector and the boiler feed the storage, which delivers the energy to the distribution system. The simulation timestep is one hour.

### Setting the load

The load imposed to the system is based on an externally simulated hourly building load. The building loads calculated utilizing the ideal heating or cooling tend to contain unrealistic peaks. Possible causes for these peaks are the strictly constant room set temperature and the lack of, in some cases very useful, conditioning of the building several hours before occupation. In a real building, it is possible to reduce or eliminate these peaks with an appropriate HVAC control system. For this reason, the peaks of the simulated load are shaved depending on their size and frequency. Usually, less than 0.2% of the timesteps are affected by the peak shaving process. The trimmed amount of energy is distributed to following timesteps where the load does not exceed the identified limit in order to maintain energy balance. The load obtained through the described process is the energy profile to be supplied by the distribution system. Furthermore, to obtain the primary HVAC system load, the building load needs to be increased to account for distribution and emission losses (secondary HVAC system losses). Since this paper focuses on the primary HVAC, we simply approximate the values of these losses relying on DIN 18599 (2007) and Olesen et de Carli (2011). This results in the primary HVAC system load.

### Boiler and thermal storage

The boiler is modelled as an ideal energy source. In each timestep during which the boiler is turned on, the boiler operates at the full load, delivering the amount of energy equal to its design power multiplied with the duration of the timestep. The energy generated by the boiler is fed to the storage, which is characterized by its volume and discharge rate. Storage volume, together with the basic differentiation between low and high temperature heating define maximal storage capacity SCmax:

$$SC \max = \begin{cases} \rho V c_p \Delta T_{high}, & \text{e.g. radiator heating} \\ \rho V c_p \Delta T_{low}, & \text{e.g. panel heating} \end{cases} \quad (1)$$

The discharge rate defines which fraction of the maximum capacity can be delivered to the load within one timestep (under condition more energy is currently stored). Apart from its role in system performance control, this value regards the physical limitations of the distribution system. Another idealization is the definition of the storage tank thermal loss to the environment. We assume a linear increase with the storage volume.

### Solar collector and solar gains

Detailed description of the solar collector model we implemented can be found in Grahovac et al. (2010).

It is based on quadratic efficiency model originating from theoretical equations developed by Duffie et Beckman (1991). The model calculates hourly solar gains as a positive part of the difference between the optical gains and thermal losses. The input data apart from the available roof area are the solar radiation incident on the latitude tilted collector surface, the angle of latitude, collector performance parameters and the average temperature of the collector fluid. The minimal amount of user input is the location and available roof area, which is the horizontal area necessary to mount the collectors. Default set of collector performance data is available for both flat plate and evacuated tube collectors in form of averaged manufacturer data. Apart from defining the thermal losses, the average fluid temperature restricts the possibility of disobeying the laws of thermodynamics by increasing the current storage capacity with the fluid of enthalpy lower than the fluid inside the storage, since we only account for the energy in this model. To determine the useful solar gain, the obtained solar gain profile is reduced for the solar system efficiency factor, representing a simplification of the solar system and storage heat exchanger losses.

### System performance control

We model a preconfigured primary HVAC system utilizing an idealized control. The goal of the control strategy is to approximate the thermal energy consumption of a real system. Although not imitating it, the control strategy in the model assumes a well done control of the real system. To avoid boiler short cycling and take advantage of the thermal storage the hysteresis has been utilized, see Fig. 3. During the process of charging the storage, the boiler stays on until one additional step of delivering the boiler full load to the storage would overflow it. After the higher limit has been reached, the boiler is turned off and the storage overtakes supplying the load, until its capacity has reached the lower limit, which is proportional to the fraction of the maximal load.

If available, solar gains are fed to the storage regardless of the boiler on-off status, until the maximum capacity has been reached. Additionally, the boiler can be turned off before the storage has been fully charged if solar gains are available. To summarize, in each of the 8760 simulation steps the boiler control signal is determined based on control and storage charge values from the previous timestep and solar gain value from the current timestep.

Depending on the current status of the system variables, a certain amount of energy (power during one timestep) can be delivered to the load:

$$D(t) = f(L(t), C(t), P, SC(t), SC_{max}, DR, SG(t)) \quad (2)$$

The storage capacity decreases for the energy discharged and increases for hourly boiler generated energy, in case the boiler was on, thus the storage capacity for the following timestep is defined:

$$SC(t+dt) = SC(t) + P \cdot C(t)dt - D(t)dt \quad (3)$$

Here we introduce the remaining load as a difference between the set and the delivered load:

$$RL(t) = L(t) - D(t) \quad (4)$$

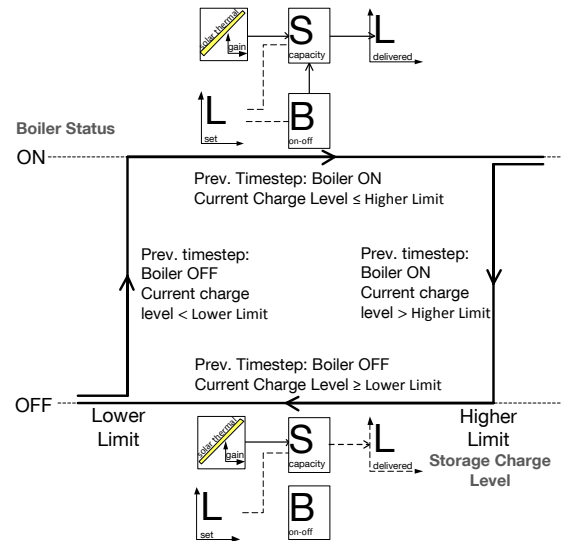


Figure 3 Boiler on-off status depends on the storage state of charge and its own previous status. This minimizes short cycling and takes advantage of the storage utilization

The remaining load has two basic functions. Firstly, it is used in defining the optimization constraint concerning the supply task. Secondly, it introduces a certain dynamics between the primary HVAC and the building simulation despite those being decoupled, allowing the active change of the set load for the following hour:

$$L(t+dt) = L(t) + RL(t) \quad (5)$$

The similarity between the model utilizing the remaining load and the real system lies in the possibility of the real system to pre-condition the building. Since this model only deals with the energy balance, supplying a certain amount of energy before or after it is due yields the same result in terms of consumption. Remaining load is illustrated in Figure 4, with further explanation in the results related chapter.

### Cost calculation

After running the simulation the array of control values for each timestep has been determined and thus the fuel consumption and CO<sub>2</sub> emissions on the yearly basis:

$$CF = \frac{P \cdot \sum C}{\eta_b} \quad (6)$$

$$E_{CO2} = CF \cdot SE \quad (7)$$

Constant boiler efficiency of 0.9 is assumed. In the current version of the model, boiler sequencing losses are neglected.

Since the dimensions of the components, as well as the fuel consumption are known, a basic cost calculation can be performed. An annuity cost calculation method prescribed by EN 15459 (2008) and VDI 2067 (2010) has been implemented. Fundamentally, total costs consist of investment costs and running costs. Investment costs consist of initial investment costs, installation costs and replacement costs, while the running costs comprise the energy and maintenance costs. An annual value which accounts for all the costs we are considering, allowing us to compare alternative designs over the same calculation period, is calculated using manufacturer and economic data together with the simulation results:

$$AC_t = f(CF, P, V, A) \quad (8)$$

Interest rate and other dynamical cost calculation parameters are considered constant during the calculation period. Risks and uncertainties of the future costs have been neglected. Since we compare different component sizes, only these components are taken into account while calculating investment, installation and maintenance costs. We assume the costs for piping, valves and other armatures, pumps etc. are equal for all alternatives and thus are not important for the comparison.

### Optimization

The usual optimization objectives in system design are costs, primary energy consumption and emissions and utilization of renewables. The objective in the example analysed in the result section of the paper is the total cost minimization, with a possibility to impose a constraint concerning the utilisation of renewables.

As obvious from eq. (5), the load will keep increasing if the system was incapable of satisfying the demand, leading to further increase in the remaining load. Thus we introduce a supply task constraint, which limits the domain of the optimization parameters excluding combinations not capable to satisfy the load. Another constraint is optional and it enables reaching of the desired solar ratio.

The objective function is simulation based, non-linear and non-differentiable. The algorithm we implemented, the Global Bounded Nelder Mead (GBNM), has proven to perform well in solving such problems (Luersen et Le Riche, 2004, Dorfner, 2010). Since it is an algorithm for non-constrained optimization, the constraints imposed to the system are transformed into non-smooth penalty functions (Nocedal et Wright, 2006). The supply penalty function tolerates occasional insufficient performance defined by the remaining load, which will not cause significant decrease of comfort. In case of the repeated high accumulation of the remaining load the penalty is activated and proportional to the sum of remaining loads. The solar penalty constraints

the solutions to those that yield the desired solar ratio. It is activated when the solar ratio is lower than its set value and scaled by the inverse of the solar ratio.

Adding the penalties to the total cost equation yields the final objective function:

$$OF = AC_t + p_{su} \sum RL + \frac{p_{so}}{SR} \quad (9)$$

Penalty parameters enable weighting of different objectives.

Since primary HVAC equipment is produced only in standardized sizes, exhaustive search of all component combinations is reasonable and quick for smaller number of discrete values and optimization variables. The advantages are the certainty of determining the global minimum, which is the major drawback of the continuous algorithm, and the possibility of parameter analyses. Clearly, with the increasing number of optimization variables an exhaustive search becomes too expensive in terms of calculation time and a more advanced algorithm is needed. Thus, this approach has been used to certify the quality of solutions yielded by GBNM algorithm.

### DISCUSSION AND RESULT ANALYSIS

Before analysing the simulation and optimization results, the data implemented for their generation are presented. We utilize simulated building load profiles, equipment price data based on curve fitting of the manufacturer data, standardized economic calculation data, idealized component efficiencies and losses and heuristic data defining the penalty functions. The data is used for the demonstration of model performance and optimization process.

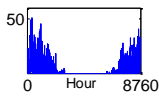
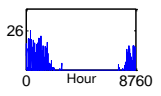
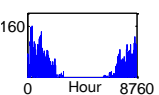
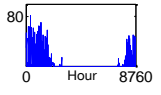
Simulated hourly building load profiles for two commercial building sizes (S for small and B for big), each for two different climates (Moscow and Shanghai weather data used), were utilized, see Table 1. Ideal heating was assumed for their generation. Building envelope is adjusted to the climate and thus different for each of the cities. For further information please refer to Liedl (2011).

The implemented value of storage thermal losses to the environment is 0.1 kW/(m<sup>3</sup>h), which is a rather optimistic interpretation of data found in Gebhardt et al. (2002).

Data concerning economic calculation, e.g. component life durations, installation and maintenance cost factors are taken from DIN EN 15459 (2007) and VDI 2067 (2010). Calculation period for the cost annuities is 20 years.

Supply and solar penalty coefficients are heuristic values satisfying the given level of investigation. These parameters weight the penalty terms and define their strictness.

Table 1 Load profiles used to demonstrate model performance

Gross Area, m <sup>2</sup> (symbol in further text)	LOCATION; LOAD PROFILE	
	Moscow; kW	Shanghai; kW
<b>1000</b> (S)		
<b>3000</b> (B)		

Since we implemented the on-off control strategy, pellet boilers are a logical choice for the analyses.

Table 2 Initial Investment cost of the components

	COSTS, €	SOURCE
Pellet Boiler	180P + 4318	Manuf. data
Thermal storage	1805.8lnV+4082.9	Gebhardt et al. (2002)
Tube Collector	414.6GA	Manuf. data

Table 3 Fuel price and emissions

PELLET	VALUE	SOURCE
Price	0.23815 €/kg	Current in DE
Emissions	0.04 kg/kWh	DIN EN 15603 (2008)

Supply and solar penalty coefficients are heuristic values satisfying the given level of investigation. These parameters weight the penalty terms and define their strictness.

The optimization variable bounds depend on the load profile and maximal roof area used as an input to the model.

The duration of one simulation (objective function evaluation) is approximately 55 ms - 11000 function evaluations can be performed within 10 minutes.

### Performance analyses

In Figure 4 we present a week of simulated model performance, with heating scheduled for the working hours. The storage tank of 2 m<sup>3</sup>, assumingly storing 120 kWh, and the discharge rate of 0.2 can cover the maximal load of 24 kW, which is the peak of the load imposed to the primary system of the building S (Table 1) in Shanghai. Highest heating demand occurs during the considered week, with low solar gains available. However, the optimal boiler power of 20kW lies beneath the peak load. During the Monday morning peak, the storage is just about to be empty and the boiler needs to supply the load. Since the full load cannot be met, the remaining load is postponed for the following timestep, and the process is continued until the full load can be supplied. The shifted load is indicated by the arrow in Figure 4. The real system would charge the storage prior to

scheduled office hours in case of low outside temperatures to avoid the lack of power, so the similarity with the real systems in terms of energy balance is achieved. The boiler stays on until the storage is fully charged and can take over the supply. Boiler cycles four times during the analysed week.

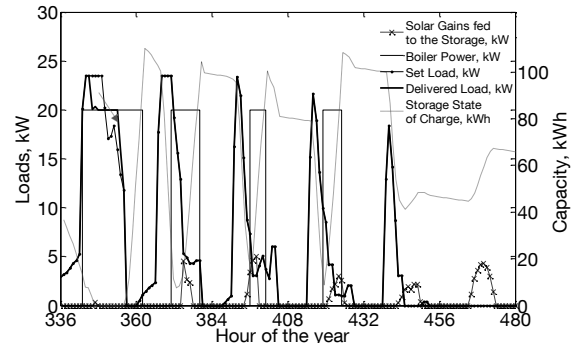


Figure 4 Model performance with optimal component sizes (Figure 9) during the third January week for Shanghai weather data and S building load.

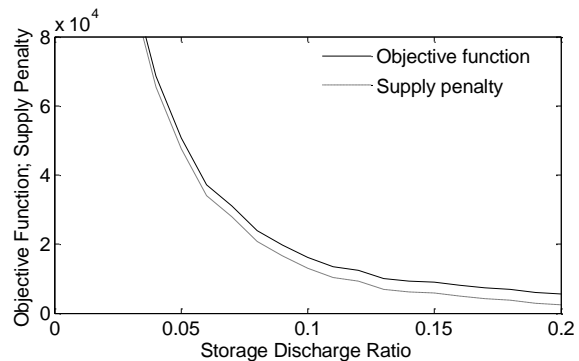


Figure 5 Systems with small storage discharge rates fail to satisfy the supply task. Moscow climate, S building, SR=0, P= 40 kW, V= 2 m<sup>3</sup>, DR= 0.2, T= 60°C.

### Analyses of the optimization results

One of the features presented in Figure 9 and Figure 10 is the comparison between the optima obtained using discrete parameters optimization and the GBNM continuous algorithm. This is done to inspect the applicability of the GBNM algorithm. Firstly, we can conclude that the differences in objective function values lie below 2%, confirming the global or very near local minima have been identified by the GBNM algorithm, thus encouraging further utilisation. Secondly, larger discrepancies in storage discharge rates are noticed. This parameter influences the performance of the system only if restriction of the hourly storage discharge is too high. This is only the case if the values are very small, such as those shown in Figure 5, or the storage volume is too small, which is usually penalized by the constraints since causing prolonged boiler operation. After the minimal satisfying discharge rate has been reached, its further increase will not change the performance. Obviously, a real system will always operate with the



lowest sufficient discharge rate, to minimize the pump size.

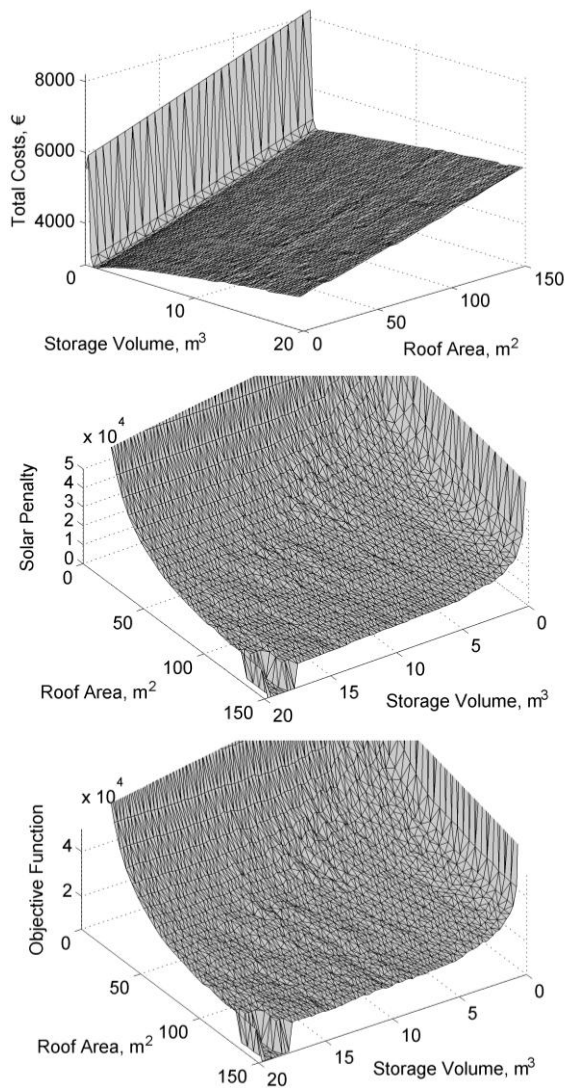


Figure 6 Objective function and its two components, solar penalty and costs for Moscow climate, S building, SR=30%, P= 35 kW, DR= 0.2, T= 60°C. Penalty forces the optimization to choose the configuration with higher costs.

In order to study the model, 3d and 2d parameter sensitivity analyses is performed. Figure 6 visualizes the objective function and its two components, solar penalty function and total costs, depending on the roof area and storage volume. Optimal values for collector temperature, boiler power and discharge rate for Moscow S building, with the demanded and reached solar ratio of 30% have been used. As expected, the total costs grow logarithmically with the storage volume and linearly with the roof area. The solar penalty, if activated, dominates the objective, posing a strict constraint which will maximize the collector size disregarding the costs. This is also seen in Figure 10 for B load in Moscow, where the penalty activation due to the insufficient solar ratio yielded maximal roof coverage with

collectors. It could be of interest to investigate a more compliant solar penalty.

Let us eliminate another dimension, slicing the 3d graphs through the optimal storage volume and optimal roof area, to investigate their influence on the objective function, costs, penalty and emissions.

Figure 7 shows the increase in annuity of the investment and total cost with the collector area. At 130 m<sup>2</sup> the desired solar ratio is achieved, removing the solar penalty. As expected, the emissions are dropping with the collector area increase. On the contrary, the emissions rise with the storage volume increase, Figure 8. To achieve a wanted temperature inside the large storage volume, the tank has to be fully charged, which prolongs the boiler working hours even if the loads would be satisfied with less energy. If imposing a constraint of achieving a certain solar ratio, while the solar penalty dominates the supply penalty, apart from collector area the storage volume will increase. In reality the process of stratification in the storage attenuates this problem.

On both Figure 7 and Figure 8 the supply penalty is due to its definitions highly non-smooth, which is a consequence of its compliant definition and dependence on the simulation performance.

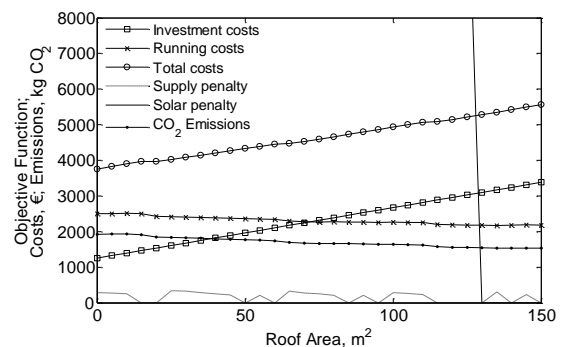


Figure 7 Moscow climate, S building, SR= 30%, P= 35 kW, DR= 0.2, T= 60°C, V=19.5 m<sup>3</sup>. Emissions decrease with the collector area.

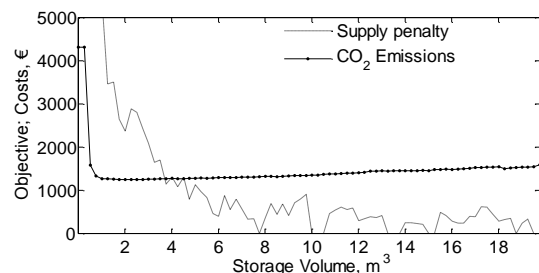


Figure 8 Moscow climate, S building, SR= 30%, P= 35 kW, DR= 0.2, T= 60°C, RA=130 m<sup>2</sup>. Emissions increase with storage volume due to the performance strategy.

Apart from comparing the two algorithms, Figure 9 and Figure 10 show an overview of optimization results for both climates and both building sizes. Clearly, the components are larger for much colder Moscow climate and thus the cost is higher. If solar

collectors are utilized, the boiler size drops and storage volume increases. The decrease in emissions is not as high as expected, due to its previously mentioned increase with the storage volume. The small inclination of the storage cost function contributes to this effect.

For all the results shown the supply task has been satisfied. The only case that penalized the solar constraint is the B building in Moscow with the objective to reach the solar ratio of 30%. Utilizing the maximal available roof area, the solar ratio of only 16.5% is achieved, and the penalty has forced the increase in storage volume, which prolonged the boiler operation hours causing the emissions to rise. For Shanghai climate, where the solar gains are higher, the boiler power decrease with the increase in solar ratio is as expected, while also the emissions are decreased.

## CONCLUSION AND OUTLOOK

A primary HVAC dimensioning procedure comprising the simplified energy balance based model, the cost calculation and size optimization has been presented.

Although highly simplified, the model is quick and yields a good estimate of the suitability, cost and performance of system configurations. Depending on desired targets, optimal configurations can automatically be determined. This has been demonstrated for a small (S) and big (B) model buildings in different climate zones (Moscow, Shanghai). The influence of environmental targets (solar ratio > 30 %) on optimal system configuration has been investigated.

Simulated results for the peak heating season week show good model performance. The postponed unsatisfied load is, if the component size allows it, covered within the following lower load hours. If this is not the case, the remaining loads accumulate, increasing the value of the supply penalty function. The supply penalty is activated if the load postponing occurs too often. The solar penalty is activated if the solar ratio is lower than desired. The optimization minimizes the annuity costs regarding the two penalties. Minimization of the objective function is performed utilizing a global bounded Nelder-Mead algorithm. The quality of the solutions has been verified by parametric runs using demonstrative building loads.

Further investigation of the model will be conducted to include the price data sensitivity analyses.

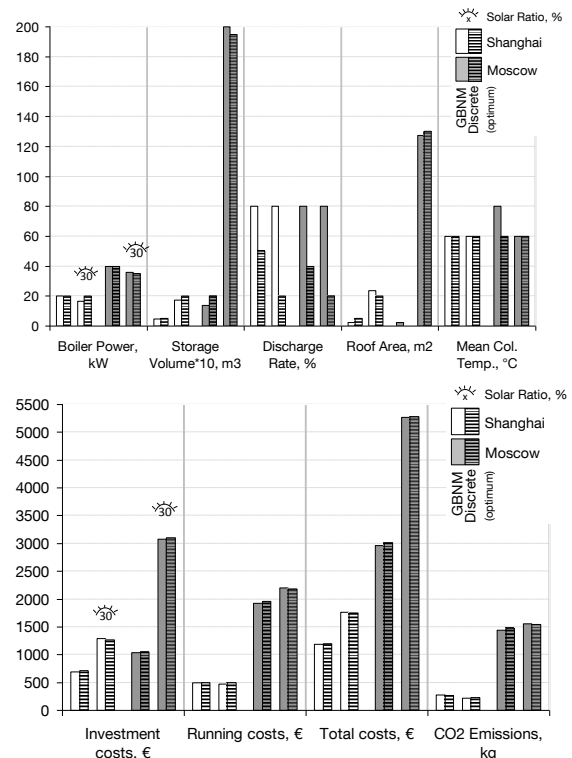


Figure 9 Optimization results for building S, both discrete and GBNM algorithms. 2<sup>nd</sup> and 4<sup>th</sup> bar of each horizontal axes variable have target SR of 30%.

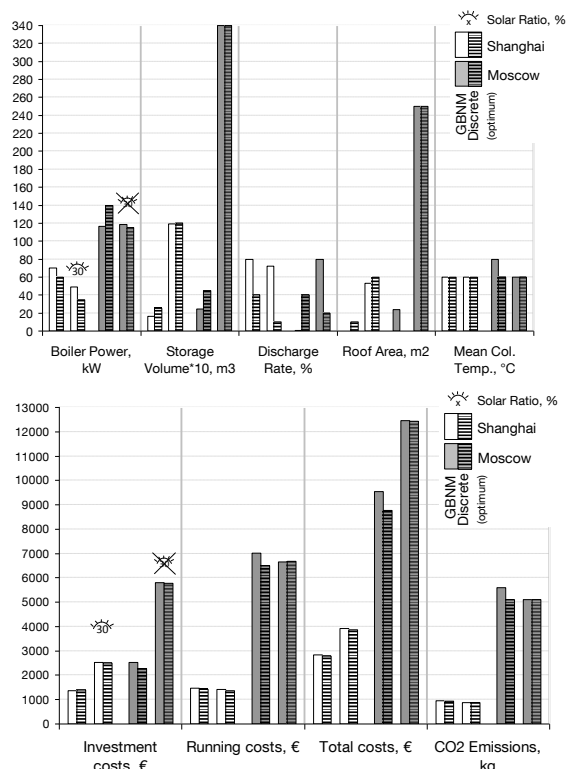


Figure 10 Optimization results for building B, equivalent to Figure 9. In Moscow climate the solar ratio of 30% has not been satisfied.

## NOMENCLATURE

SC <sub>max</sub>	maximal storage capacity, kWh
$\rho$	Water density, kg/m <sup>3</sup>
V	Storage volume, m <sup>3</sup>
$\Delta T$	Storage temperature difference, °C
D	Load delivered to the distrib. system, kW
L	Load imposed to the plant, kW
C	Boiler control signal, 0 or 1
P	Boiler design power, kW
SC	Storage capacity, kWh
DR	Storage discharge rate
SG	Solar gain, kW
RL	Remaining load, kW
CF	Consumed fuel, kWh
$\eta_b$	Boiler efficiency
E <sub>CO2</sub>	CO <sub>2</sub> emissions, kg/a
SE	Specific emissions, kg/kWh
AC <sub>t</sub>	Total annuity costs, €
RA	Roof area under collectors, m <sup>2</sup>
GA	Gross collector area, m <sup>2</sup>
P <sub>su</sub>	Supply penalty coefficient
P <sub>so</sub>	Solar penalty coefficient
SR	Solar ratio
t	Time, hourly resolution

## REFERENCES

- CIBSE TM38. 2006. Renewable energy sources for buildings.
- DIN 18599:2007. Energetische Bewertung von Gebäuden.
- DIN EN 15459:2008. Energieeffizienz von Gebäuden - Wirtschaftlichkeitsberechnungen für Energieanlagen in Gebäuden.
- DIN EN 15603:2008. Energieeffizienz von Gebäuden- Gesamtenergiebedarf und Festlegung der Energiekennwerte.
- Dorfner, J. 2010 Development of a Simulation Tool for Renewable Hydrogen Supply of Fuel Cell Vehicles, Diploma Thesis, Technische Universität München.
- Duffie, J.A., Beckman, W.A., 1991. Solar Engineering of Thermal Processes, John Wiley & Sons, Inc., New York ISBN 0-471-51056-4.
- Fabrizio, E., Filippi, M., Virgone, J. 2009. An hourly modelling framework for the assessment of energy sources exploitation and energy converters selection and sizing in buildings, Energy and Buildings 41, Nr. 10 1037-1050.
- Gebhardt, M., Kohl, H., Steinrötter, Th. 2002. Ableitung von Kostenfunktionen für Komponenten der rationellen Energienutzung, Institut für Energie- und Umwelttechnik e.V. (IUTA).
- Grahovac, M., Liedl, P., Frisch, J., Tzscheutschler, P. 2010. Simplified Solar Collector Model: Hourly Simulation of Solar Boundary Condition for Multi-energy Optimization, In Proceedings of 41st International HVAC&R congress Belgrade, Serbia.
- Hirsch, J. 2006. eQuest. The Quick Energy Simulation Tool.
- Lambert, T., Gilman, P., Lilienthal, P. 2005. Micropower system modeling with HOMER, Integration of Alternative Sources of Energy, Farret FA, Simões MG, John Wiley & Sons.
- Liedl, P. 2011. Interaction Climate-Human-Building: Planning tools for office buildings in different climate zones in the context of room climate and energy with a detailed climate analysis, Dissertation at TUM.
- Luersen, M. A., Le Riche, R. 2004. Globalized Nelder-Mead method for engineering Optimization, In ICECT'03: Proceedings of the third international conference on Engineering computational technology, Edinburgh.
- Nocedal, J., Wright, S. 2006. Numerical Optimization, Springer.
- Olesen, B., de Carli, M. 2011. Calculation of the yearly energy performance of heating systems based on the European Building Energy Directive and related CEN standards, Energy and Buildings 43, 1040-1050.
- Sakurai F., Inooka, T., Yanagihara, R., Higashizawa E, Hamane, J., Fujii, T., Nishihata, H., Hayashi, H., Arizumi, F, Ninomiya, H., Koike, K., Shinohara, N. 2007. FACES (Forecasts of air-conditioning system's energy, environmental, and economical performance by simulation), Proceedings of Building Simulation 2007, Beijing.
- VDI 2067:2010. Blatt 1 Wirtschaftlichkeit gebäudetechnischer Anlagen - Grundlagen und Kostenberechnung.